Dynamic optical tomographic imaging of the human forearm for quantification of the vascular bed response in diabetics and non-diabetics

Nelson A. Franco[1], Rosemarie E. Hardin[1], Michael S. Katz[1], David P. Klemer[2], Harry L. Graber[2], Christoph H. Schmitz[2], Stephanie Lum[2], MaryAnn Banerji[3], Alessandro G. Smeraldi[4], Thomas F. Panetta[4] and Randall L. Barbour[2]

Departments of Surgery[1],Pathology[2] and Medicine[3], SUNY Downstate Medical Center, 450 Clarkson Avenue, Brooklyn, New York 11203

Department of Vascular Surgery[4], Staten Island University Hospital, 475 Seaview Avenue, Staten Island, New York 10305

INTRODUCTION

Associated presentations and previously published work [1,2] have laid out the principles and physiological rationale for dynamic near-infrared optical tomography (DYNOT), a functional imaging method that we expect will prove highly effective for noninvasive examination of the spatiotemporal dynamics of the vascular response [1]. This optical technique does not require invasive procedures such as venipuncture or angiography, or exposure to known harmful radiation or to nephrotoxic dyes.

The clinical utility of an imaging modality sensitive to vascular response dynamics stems from the ubiquity of microvessels in tissue and the near certainty that derangements of their normal rhythms will occur in conjunction with pathological states. A significantly prevalent specific example is Type 2 diabetes, which leads to many well-characterized abnormalities of peripheral blood vessel walls [3–5]. Consequently, the primary hypothesis underlying the study reported on here is that one can noninvasively evaluate vascular pathophysiology associated with Type 2 diabetes (DM2) by means of a DYNOT measurement. It is found that a mild temperature-shock provocation—ca. 10 min. of warming the skin to a temperature of 37.8-40.6 °C with a heating pad—readily permits us to discriminate between healthy control subjects (euglycemics) and patients with DM2. This was the finding that had been predicted, based on the loss of the normal peripheral vasodilatory response to local tissue heating that is known to occur in DM2.

In addition, we have found a strong relationship between an accepted measure of glycemic control in diabetics (glycosylated hemoglobin) and our optical measurements of vascular dynamic changes. This suggests the possibility of eventually replacing the invasive clinical test performed at present with a DYNOT-based noninvasive imaging technique. As a general matter, clinical adoption of near-infrared optical techniques in diabetes management would offer significant advantages over conventional approaches: (1) measurements are done in real time, (2) they are noninvasive, and (3) they may obviate the need for multiple repeated blood draws.

METHODS

Data Collection

Optical tomographic measurements were performed with the NIRx DYNOT imager configured for 24 illumination sites and 24 detection channels resulting in 24² = 576 data acquisition channels. The acquisition rate was 2.5 frames per second, and dual-wavelength illumination (760 and 830 nm) was employed to distinguish the hemoglobin (Hb) oxygenation states. The instrument was equipped with a circular measuring head (Fig. 1) for limb imaging, which allows for pneumatically controlled radial fiber translation to achieve easy measurement setup and good fiber contact over a wide range of target sizes.

Before the measurement, each subject was attached to the following vital signs monitors: 3-lead EKG, Pulse Oximeter, and Radial Artery Tonometer. A blood pressure cuff was placed around the subject's left arm, and a heating pad was positioned around the forearm proximal to the optical probes. The volunteer was then placed in a reclining seated recumbent posture, and remained at rest during the measurements. The left arm of the subject was pronated and placed inside the iris measurement head, and the fiber optics were adjusted (Fig. 1). The volunteer was allowed to acclimate to his/her position in the chair and the environment for twenty minutes before any experimental provocations were initiated.

Twenty three volunteers were measured; 40% were female, 60% were ethnic minorities. Volunteer ages ranged from 18 to 68. Nine of the volunteers were clinically diagnosed moderately to well-controlled diabetics receiving only oral therapy (mean HbA_1c <8%). Of the patients diagnosed as diabetics, most had a duration of diagnosis greater than five years. Diabetic volunteers were already cross-enrolled in a medicine study program that carefully monitored their health, thus giving us access to their blood chemistry results.

Experimental provocations consisted of inflation of the blood pressure cuff on the left arm to a pressure of 60mmHg to induce venous occlusion. This provocation was performed 4 times. The provocation lasted 80 seconds, with 160 seconds between each provocation. The volunteer's left forearm was then gently warmed with a digitally controlled, clinically approved warming pad to a temperature of 105°F. After 10 minutes, 4 venous occlusion provocation measurements were again performed on the warmed arm. For one patient, the venous occlusion was performed only (no arm heating) with the arm in the supine position and in the prone position.

Data Analysis

Once measurements were acquired, the data was processed with the *dynaLYZE* software package.

1. Data pre–processing. Raw data for all channels that passed the data-integrity checks were normalized based on the time-varying laser intensity recorded during the experiment, then were further normalized based on the mean value recorded during the baseline period. During this step, an adaptive median filtering algorithm was applied, as needed, to eliminate negative instantaneous values resulting from measurement noise.

2. Image Reconstruction. Image recovery was achieved using the Normalized Difference Method [2]. As previously shown, this algorithm is markedly insensitive to expected uncertainties in boundary conditions, which are unavoidable in experimental methods. A truncated singular value decomposition procedure is used to solve the linear perturbation equation. The absorption coefficient images were subsequently post-processed to produce image time series for oxygenated, deoxygenated, and total hemoglobin (Hb) concentration changes. For the reconstructed image time series, the changes in Hb concentration (Fig. 2) were computed from the reconstructed two-wavelength absorption coefficients at each FEM mesh node, by solving a simple algebraic system of two equations in two unknowns. For the detector readings time series, relative concentration changes for the Hb states were estimated via a modified Lambert-Beer law.

3. Signal Analysis. 1) A general linear model (GLM) algorithm was applied to the detector data or the image time series to find the best fit of each time series to a model function created by spatially averaging over all source-detector pairs or, in the case of reconstructed images, over all pixels in each image. The GLM method is schematically illustrated in Fig. 3. The analysis yields the fitting parameters (GLM coefficients) for each data channel or image pixel, as well as the percentage of variance accounted for (PVA) in each channel's or FEM mesh node's time series. 2) A rate analysis strategy was employed to quantify changes in vascular compliance by judging the transient response of the optical signal to the occlusion maneuver in absence and presence of a heating stimulus. This analysis employed measures of the steepness in the transient rise ("upslope") and fall ("downslope") of the optical signal, as well as the temporal width of the signal response. In addition, the integrated area under the signal curve during the response interval was used as a measure of the response strength.

RESULTS

Method Validation

Fig 2 shows two oxy-Hb spatial maps that were computed from two-wavelength reconstructed absorption-coefficient images, starting with data collected during a venous occlusion protocol without heating. Plotted are spatial maps of GLM coefficients, for a model function that consisted of the spatially averaged detector response.

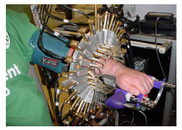

Fig. 1: Photograph of typical placement of volunteer's arm in the Iris Imaging Head and placement of BP Cuff for venous occlusion provocation. Obscured from view is the heading pad.

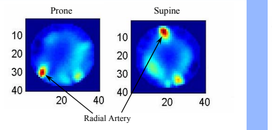

Fig. 2: Recovered optical images of the oxyhemoglobin signal for prone and supine orientations of the forearm of a healthy volunteer.

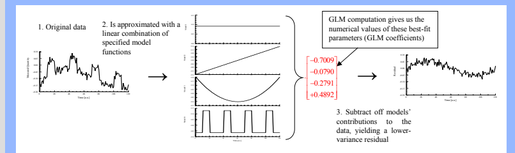

Fig. 3: Schematic illustration of the action of a GLM computation.

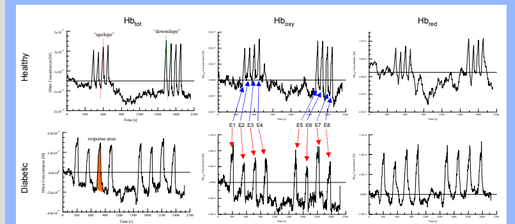

Fig. 4: Time courses of the spatially averaged image data for three hemoglobin states. Top row: healthy subject, bottom row: diabetic patient. Indicated are some of measures employed in our rate analysis.

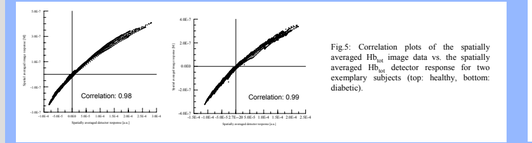

Fig.5: Correlation plots of the spatially averaged Hb_{tot} image data vs. the spatially averaged Hb_{tot} detector response for two exemplary subjects (top: healthy, bottom: diabetic).

They represent two subsequent measurements on the forearm of a healthy volunteer, one with the forearm pronated and the other with the forearm supinated. These results validate our measurement and analysis approach and demonstrate our ability to distinguish between components of the vascular tree. Since oxy-Hemoglobin is carried in the arterial circulation, the maximum signal is presumed to originate from the major arteries, most likely the radial artery. In agreement with this expectation, we find in both cases that the signal maximum coincides with the physical location of the radial artery, according to the known orientation of the arm.

Fig. 4 shows the spatially averaged time courses of detector data for one healthy and one diabetic subject for the occlusion/heating protocol described above. Occlusion epochs E1-E4 were carried out before heating of the arm, and E5-E8 were performed after. Whereas heating causes a marked change in the signal response to occlusion for the healthy subject, suggesting increased vascular compliance, this response is blunted in the diabetic volunteer. This behavior, which suggests impeded vascular reactivity for the diabetic subject, in agreement with the known pathology of diabetics, is a result consistently observed throughout our study.

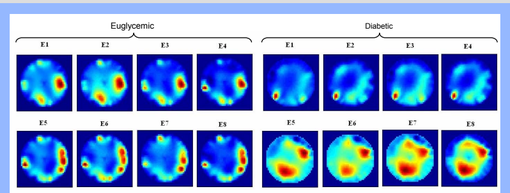

Fig.6: GLM maps of change in Hb_{tot} concentration for one healthy and one diabetic subject. Epoch 1 (E1) – Epoch 4 (E4), vaso-occlusion before warming, E5-E8, after warming.

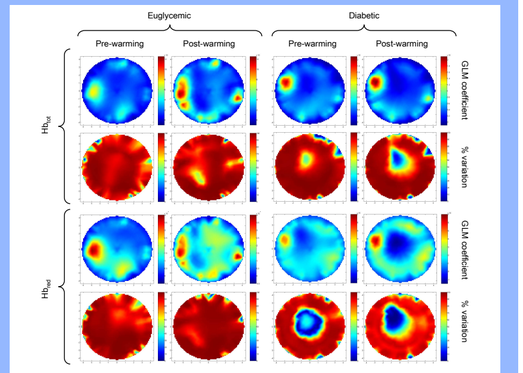

Fig.7: Spatial maps of the GLM coefficients and percentage-of-variance-accounted-for-by-the-model-function (PVA) values, for one healthy and one diabetic subject.

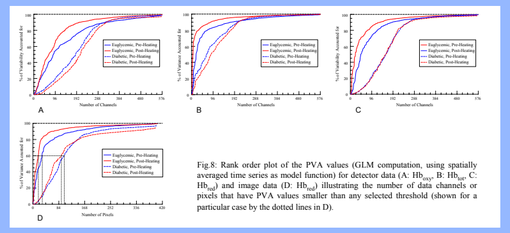

Fig.8: Rank order plot of the PVA values (GLM computation, using spatially averaged time series as model function) for detector data (A: Hb_{oxy}, B: Hb_{tot}, C: Hb_{red}) and image data (D: Hb_{tot}) illustrating the number of data channels or pixels that have PVA values smaller than any selected threshold (shown for a particular case by the dotted lines in D).

To validate our confidence in the reconstructed image time series, we compared the average detector data signal with the time series of the spatially averaged image pixel values, and found them qualitatively very similar. This is demonstrated by correlation plots in Fig. 5, which, while not perfectly linear, demonstrate that the detector and image data are strongly positively correlated.

GLM Results

Fig. 6 shows spatial maps of the GLM coefficients for the Hb_{tot} signal, for each of the occlusion epochs, of one diabetic and one healthy subject. The cuff occlusion provocation causes vasoengorgement, leading to an increase in both Hb states. Gentle heating is applied between E4 and E5 to study changes in vascular compliance during the occlusion. The healthy subject shows a focused response to heating, primarily occurring in the superficial microvasculature, whereas the diabetic's response is more diffusely distributed throughout the volume of the arm.

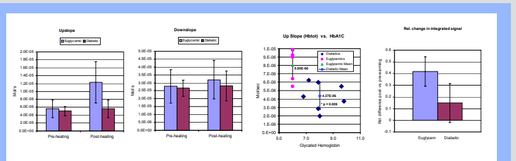

Fig. 9: Rate analysis results; comparison of the signal upslope (A) values and downslope (B) values for euglycemic and diabetic subjects, pre- and post warming. Plotted are the mean gradient values for linear fits, on multiple subjects. Error bars indicate standard deviation. C) Relation between upslope steepness and HbA1C level. D) Comparison of the change in the integrated signal during occlusion after warming, relative to the integrated response at ambient temperature (i.e., pre-warming), for euglycemic and diabetic subjects. Shown are the mean values for multiple subjects. Error bars indicate standard deviation.

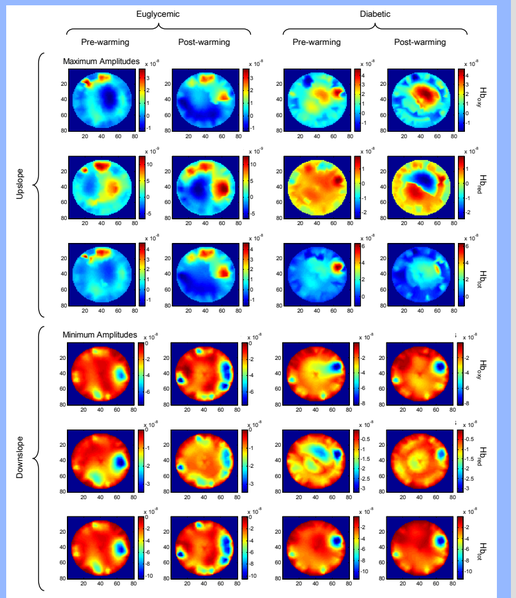

Fig. 10: Spatial maps of the maximum (upslope) and minimum (downslope) gradient values for one representative euglycemic and one representative diabetic subject. The pre-warming results were obtained from E1, and the post-warming result was obtained from E5.

Rate Analysis

Another approach to analyzing differences in the physiologic responses of diabetics and euglycemics to venous occlusion, and the effect of local tissue heating on these responses, was to quantify the rate of transient changes in detector and image time series. The elementary method adopted was to measure the steepness of the rising ("upslope") and the falling ("downslope") of the response curve, either by calculating the gradient of a linear fit or by locating the extrema of the numerical derivative curves. Fig. 9-A compares the change in the Hb_{tot} upslope, of the reconstructed image series, for both subject groups. The slopes for all epochs were obtained through linear fitting and were averaged for all pre-heating epochs and post-heating epochs to obtain an average pre- and post-heating slope per subject. Fig 9-A shows the mean and standard deviation (STD) for those results. The same procedure was applied to the downslopes, and the results are displayed in Fig. 9-B. Because of inconsistencies in the protocol, some subjects had to be excluded, and these analyses were performed on only a limited number of subjects.($n_{healthy}$ = 2, $n_{diabetic}$ = 6). The post-warming upslope difference between volunteer groups was found to be statistically significant (unpaired t-test probability = 0.031). There was no statistically significant difference in the other slope values.

In addition to the slope analysis, we quantified the change in area under the response signal curves as a measure of response magnitude. Although this is an even grosser measure than the slope analysis, as an integral method, it promises to be intrinsically more stable and less sensitive to noise.

Fig. 9-C shows the relation between the upslope analysis results and the HbA1C values of the subjects as a measure of disease severity. Since HbA1C value were available only for the diabetics, a value of 6.0 was assumed for all healthy subjects. The upslopes for the euglycemic volunteers show a mean value of 8.00E-6 M/s, while the diabetic group are clustered around an average HbA1c value of 8.0, with an average upslope of 4.37E-6 M/s. These findings suggest a correlation between the presence and severity of diabetes and the optically measured suppression of vascular regulation. The findings are statistically highly significant (p=0.009).

Fig. 9-D shows the relative difference between the integrated signal responses of the reconstructed image time series (H_{tot}) for the post-heating epochs compared to those of the pre-heating epochs. The spatially integrated image series were integrated for each epoch individually, and the results were averaged over all pre-heating epochs and all post-heating epochs, for each subject. The relative change in area *A* of the average post-heating response with respect to the pre-heating response was calculated for each subject ($[A_{post}- A_{pre}]/A_{pre}$). Graphed are the averaged results for each subject group (mean and STD, $n_{healthy}$ = 3, $n_{diabetic}$ = 7). We observed a statistically significant difference for the increase in response strength between the two groups (unpaired t-test probability = 0.037). Euglycemics show an average increase of 42% in the Hb_{tot} response to occlusion after warming, whereas for diabetics this value is 15%.

Fig. 10 shows imaging results derived from the rate analysis. Shown are the spatially mapped magnitude of concentration changes in the forearm resulting from venous occlusion before (E1) and after (E5) heating for a healthy and a diabetic person. Mapped are the upslope and downslope, obtained via the numerical differentiation technique, in each pixel of the image series, for all Hb states. As in the GLM results, the heating causes a more focused response to the heating maneuver in the euglycemic, while in the diabetic the changes are more diffuse.

CONCLUSIONS

Time series imaging of the hemoglobin signal provides a simple and direct means to explore vascular changes in the periphery in response to a transient hemodynamic challenge. The responses seen, both to mild heating and to induction of mild venous congestion, provide for repeatable responses (+- 10-15%) in amplitude and contrast features of the cross-sectional maps. Comparison of optical rate metrics and HbA1C levels show that the two are significantly correlated even in well-controlled diabetics suggesting that DYNOT measures of the periphery may serve as a suitable noninvasive surrogate for monitoring the long term effects of diabetes on the peripheral vasculature.

REFERENCES

[1] R. L. Barbour, H. L. Graber, Y. Pei, S. Zhong, and C. H. Schmitz, "Optical tomographic imaging of dynamic features of dense–scattering media," J. Opt. Soc. Am. A 18, 3018–3036 (2001).

[2] Y. Pei, H. L. Graber, and R. L. Barbour, "Influence of systematic errors in reference states on image quality and on stability of derived information for DC optical imaging," Appl. Opt. 40 5755–5769 (2001).

[3] K.B. Stansberry et al., "Impaired Peripheral Vasomotion in Diabetes," *Diabetes Care,* 19: 715-721(1996)

[4] K.B. Stansberry et al., "Impaired Peripheral Vasomotion in Diabetes," *Diabetes Care,* 19: 715-721(1996)

[5] The Diabetes Control and Complications Trial Research Group. " The absence of a glycemic threshold for the development of long-term complications: the perspective of the Diabetes Control and Complications Trial." *Diabetes* 1996; 45:1289.

ACKNOWLEDGMENTS

This research was support in part by the National Institutes of Health (NIH) under Grants R21-HL67387, R21-DK63692 and R41-CA96102.

Fig. 7 illustrates the different response of a healthy and a diabetic subject to the occlusion/warming protocol. Shown are the GLM coefficient maps for the reconstructed Hb_{tot} and Hb_{red} images series for E1 (pre-warming) and E5 (post-warming) with their respective confidence maps. Again, the reaction to heating is more pronounced and more spatially focused in the healthy subject than it is in the diabetic in agreement with the known physiology and pathology. The confidence maps demonstrate that a large percentage of the temporal variance in most pixels can be attributed to the model function that was used.

The difference in the spatial coordination (homogeneity) of the vascular responses of euglycemics and diabetics, as seen in the spatial maps in Fig. 7, is more quantitatively illustrated in Fig. 8.

Shown here is the percentage of variance accounted for (PCA value), ranked in order from smallest to largest, in all detector channels or image pixels. The steeper the initial rise of these curves, the more spatially coordinated the response is, because few regions have hemoglobin state time series that are substantially different from the spatially averaged behavior. It can be seen that for the diabetic, the curves for both Hb states shown are consistently more shallow in their initial slope, indicating a greater degree of spatial heterogeneity than in the healthy subject.

I look to ***THE DIFFUSION OF LIGHT*** and education as the resource to be relied on for ameliorating the condition, promoting the virtue, and advancing the happiness of man.

— Thomas Jefferson (1822)